frontiers | Frontiers in Energy Research

TYPE Original Research
PUBLISHED 14 November 2024
DOI 10.3389/fenrg.2024.1503787

OPEN ACCESS

EDITED BY
Jinlong Liu,
Zhejiang University, China

REVIEWED BY
Tianfang Xie,
Purdue University, United States
Junqing Zhu,
ExxonMobil Research and Engineering, United States
Nan Zhang,
University of West Florida, United States

*CORRESPONDENCE
V. Mahendra Reddy,
mahendra@iitkgp.ac.in
Giancarlo Sorrentino,
giancarlo.sorrentino@stems.cnr.it

RECEIVED 29 September 2024
ACCEPTED 31 October 2024
PUBLISHED 14 November 2024

CITATION
Srinivasarao M, Sorrentino G and Mahendra Reddy V (2024) Investigation of the interaction of the MILD regime with HiTAC and no-combustion regimes in combustion region diagrams.
Front. Energy Res. 12:1503787.
doi: 10.3389/fenrg.2024.1503787

Investigation of the interaction of the MILD regime with HiTAC and no-combustion regimes in combustion region diagrams

M. Srinivasarao[1], Giancarlo Sorrentino[2]* and V. Mahendra Reddy[1]*

[1]Combustion Chemical Kinetics Research Laboratory (CCKRL), Mechanical Engineering, Indian Institute of Technology Kharagpur, Kharagpur, India, [2]Institute of Science and Technology for Sustainable Energy and Mobility (STEMS), National Research Council (CNR), Naples, Italy

Moderate or intense low-oxygen dilution combustion is vital for reducing emissions. Recent advancements have introduced regime diagrams for various reactant mixtures, highlighting no-combustion, Moderate or intense low-oxygen dilution, and high-temperature air combustion regions to analyze the overall operating range. However, studies on these diagrams are limited and often lack detailed analysis. This study focuses on the interaction of the Moderate or intense low-oxygen dilution regime with other regimes, particularly examining ignition delay time. Initially, ignition delay times are analyzed using regime diagrams for methane, propane, and syngas fuel mixtures. Calculations reveal a consistent ignition delay time range at the boundary between Moderate or intense low-oxygen dilution and no-combustion, varying with fuel type. To investigate further, combustion regime diagrams for methane and methane-hydrogen mixtures are developed, considering dilution levels and preheating effects with N_2, CO_2, H_2O, and exhaust gas recirculation. These diagrams examine the spread of the Moderate or intense low-oxygen dilution regime and the ignition delay times at the boundaries. The upper and lower limits of the moderate or intense low-oxygen dilution regime are noted based on obtained ignition delay times. An emission-based analysis within these regimes is conducted to assess the effectiveness of techniques in achieving moderate or intense low-oxygen dilution combustion. Proposed ignition delay time range for the considered mixtures aims to maintain mixture within the moderate or intense low-oxygen dilution regime, ensuring lower emissions. This is also further proved with the numerical simulations. The study also explores the sensitivity of dilution level, mixture temperature, N_2, CO_2, H_2O, and EGR on the Moderate or intense low-oxygen dilution regime.

KEYWORDS

combustion regime diagrams, MILD combustion, ignition delay time, emissions, chemkin

1 Introduction

Due to the substantial rise in fossil fuel usage for combustion applications, emissions have notably increased. In response to stringent pollution regulations and concerns over emissions from conventional combustion, low-emission technologies such as high-temperature air combustion (HiTAC) (Katsuki and Hasegawa 1998), flameless oxidation (FLOX©) (Wünning and Wünning, 1997), and colorless distributed combustion (CDC) (Arghode and Gupta 2011) have been developed (de Joannon et al., 2012; Sabia et al., 2021; Sorrentino et al., 2015). The moderate or intense low-oxygen dilution (MILD) combustion technique operates similarly to these technologies but with a different mode of operation, offering greater flexibility regarding various energy vectors (Ariemma et al., 2023; Garnayak et al., 2022; Garnayak et al., 2023; Sorrentino et al., 2017). MILD combustion involves supplying the reactants at a temperature higher than the reactant mixture's self-ignition temperature while ensuring that the temperature rise within the combustor remains below the self-ignition temperature of the fuel. MILD combustion ensures a more uniform distribution of the flame, thereby reducing significant temperature gradients within the combustor. This results in lower emissions and higher efficiency. MILD combustion flames operate under lower oxygen concentrations or higher exhaust gas recirculation, making them significantly different from conventional flames. Due to these conditions and the lower operating temperatures, maintaining flames within the MILD combustion regime is challenging (Mardani and Fazlollahi Ghomshi, 2016; Srinivasarao and Reddy 2024). Consequently, MILD combustion flames have attracted significant attention for their potential, which is being explored through computational and experimental analyses. Several computational simulations (Christo and Dally 2005; Darbyshire and Swaminathan 2012; Giuntini et al., 2023; Srinivasarao et al., 2023) and experiments (Galletti et al., 2017; Kumar et al., 2002; Mahendra Reddy et al., 2013) have been conducted to understand the challenges in achieving MILD combustion for various fuels. In addition, different combustion regime diagrams were constructed for methane (de Joannon et al., 2012; Garnayak et al., 2022; Rao and Levy 2010), propane (Sorrentino et al., 2016), syngas (Kim et al., 2021), and enriched syngas (Kim et al., 2021) to assess the feasibility of MILD combustion across a wide range of oxygen concentrations and preheating temperatures.

Combustion regime diagrams provide a fundamental understanding of reactive region characteristics under different dilution and preheating conditions. The combustion regime diagram typically consists of three regions namely, (i) no-combustion regime in which the combustion process is not initiated (ii) MILD regime where the temperature difference between the peak temperature (T_{peak}) of the flame and reactants temperature (T_{mix}) is less than that of the self-ignition temperature ($T_{ignition}$) of fuel ($\Delta T = T_{peak} - T_{mix} < T_{ignition}$) (iii) HiTAC regime where ΔT is higher than that of the self-ignition temperature ($\Delta T > T_{ignition}$) and $T_{mix} > T_{ignition}$. Nevertheless, several criteria have been put forth in the literature to define the characteristics of MILD combustion. Three major criteria to identify the MILD combustion regime are (i) ΔT criteria: the definition is more towards the ignition point of the reactants and temperature increment in the combustion process proposed by Cavaliere and de Joannon (2004), mathematically, $\Delta T = T_{peak} - T_{mix} < T_{ignition}$ (ii) heat release rate criteria: heat release rate profiles that present in the burner a single positive peak without any negative values are symptomatic of MILD combustion (Sorrentino et al., 2021) (iii) K_v criteria: the K_v criteria quantifies recirculation within the burner, primarily relying on the recirculation ratio (Reddy et al., 2015; Sharma et al., 2018). It serves to distinguish various combustion regimes in burners with confinements. Kv is a recirculation factor is defined as ratio of the recirculated gases. This value is also well defined in the literature that Kv = 4 for methane and Kv = 3 for ethane fuels for achieving the MILD combustion (Cavigiolo et al., 2003). Other criteria were also used in the literature, such as the disappearance of extinction phenomena while varying mixture dilution levels (Sabia et al., 2023), through the identification of the condition where ignition and extinction collapse in a unique event (Reddy et al., 2015).

Most of the combustion regime diagrams created in the literature are based on the definition given by Cavaliere and de Joannon (2004). Hence, the borderline between the HiTAC and MILD combustion regimes is associated with the definition of MILD combustion, i.e., $T_{peak} - T_{mix} < T_{ignition}$. However, the flame is well stabilized in both HiTAC and MILD regimes. The interaction between the MILD regime, HiTAC, and no-combustion regimes is crucial, as it maintains a nearly consistent ΔT range. Additionally, when the reactive region transitions from the no-combustion to the MILD combustion regime, combustion properties undergo significant changes. Therefore, these interactions should be examined using a parameter that encapsulates all operational factors and is highly sensitive to the combustion process. Ignition delay time (IDT) is selected as a prominent parameter in the current study to understand the underlying physics of various combustion regimes and their interactions.

The characteristics of the reactant mixture can be identified using ignition delay time (IDT). Studies on IDTs for methane (Ebrahimi Fordoei and Mazaheri, 2021; Garnayak et al., 2022; Tu et al., 2020) and propane (Sabia et al., 2015; Yang et al., 2022) under various pressures, preheating temperatures, and combustion dilution percentages have shown that MILD combustion phenomena are particularly sensitive to IDT. A rapid change in IDTs occurs when transitioning from no-combustion to the HiTAC regime, and a similar trend is observed when reactant properties moving from no-combustion to the MILD regime. However, the IDT variation is less pronounced during the shift from no-combustion to the MILD regime. Such variation in IDTs when the flame is shifting from one regime to another regime is not discussed in the literature.

In the present work, ignition delay times (IDTs) of various combustion regimes are studied, initially focusing on the flame transition from the no-combustion regime to the MILD regime. Several data points on the borderline between the MILD and no-combustion regimes are considered, and IDTs of the selected data points are thoroughly analyzed. In the primary investigation, it is observed that the IDTs at the borderline points between the MILD and no-combustion regimes exhibited similar range of magnitudes for a given fuel mixture, though this magnitude varied depending on the fuel mixture. Based on this insight, a comprehensive examination is conducted focusing on the methane fuel regime diagrams. This investigation encompassed various conditions, including hydrogen blending, preheating, and dilution

with CO_2, H_2O, O_2, and EGR. Combustion regime diagrams for methane and methane-hydrogen using a plug-flow reactor (PFR) in Chemkin Pro are developed. These diagrams are considered for analyzing the borderline points between the MILD and no-combustion regimes, as well as the MILD and HiTAC regimes. Additionally, an emission analysis for CO and NO within these regime diagrams is conducted. Furthermore, the influence of various techniques employed in achieving MILD combustion is investigated.

2 Preliminary analysis of the borderline between MILD and no-combustion regime

Data for the reacting mixtures are being analyzed to understand the characteristics of reactant mixtures across various combustion regimes and their borderlines. This section primarily focuses on characterizing the designated borderline points between the MILD and no-combustion regimes. For the analysis purposes, various regime diagrams from existing literature, specifically those for methane, propane with CO_2 and H_2O dilution, syngas, and enriched syngas, are being considered. Within each of these combustion regime diagrams three data points in each regime (no-combustion, HiTAC, and MILD) and seven points located along the border between the no-combustion and MILD regimes, are extracted. Subsequently, the ignition delay times (IDTs) are calculated for these extracted data points.

2.1 Selection of combustion regime diagrams

Figures 1A, B illustrate the combustion regime diagrams for methane fuel under O_2 dilution (Garnayak et al., 2022) and exhaust gas recirculation (EGR) (Rao and Levy 2010), respectively. These regimes are developed by varying the O_2 concentration in the oxidizer and the unburned mixture temperature. As discussed previously, the selected points are denoted by dots and numbered accordingly. The first group (1–3) falls within the no-combustion regime, the second group (4–10) lies on the borderline between the no-combustion and MILD regimes, the third group (11–13) is situated in the MILD regime, and the last group (14–16) is within the HiTAC regime. This numbering system is maintained consistently throughout this section.

The complete mixture composition and operational parameters are collected for the selected points, which are utilized in numerical simulations to calculate the ignition delay times (IDTs). Figures 2A, B depict the combustion regimes for propane fuel with CO_2 and N_2 dilutions, established using the reactant temperatures and C and O radicals' ratio in the reactant mixture (Sorrentino et al., 2016). Figures 2C, D show combustion regime diagrams for syngas and enriched syngas based on mixture temperatures and oxygen dilution (Kim et al., 2021).

The regime diagrams illustrating different combustion regimes for the fuels reveal that MILD regimes are stable within an oxygen dilution range of 1.5%–9%. However, the temperature ranges differ according to the flammability of the fuel and oxidizer mixture. This indicates that the reduction in oxygen concentrations in the reactant mixtures is compensated by the reactant temperatures. Notably, CO_2 dilution enhances the MILD-operated regime when compared with the N_2 diluted MILD regime for the case of propane (Figures 2A, B). Additionally, hydrogen enrichment of syngas enhances the MILD regime (Figures 2C, D). The detailed analysis of the extracted points is well explained in the IDT calculation section.

2.2 Ignition delay times calculation

Numerical simulations are conducted using detailed chemistry for the respective fuel with a closed homogeneous reactor present in Chemkin Pro. In the closed homogeneous reactor, the ignition delay time (IDT) is defined as the duration in which the combustion process releases the maximum amount of heat, indicated by the inflection point in the temperature profile. Alternatively, it can be determined as the time corresponding to the peak concentration of a specific species chosen by the user, often the OH mass fraction (Srinivasarao et al., 2024; Mardani and Karimi Motaalegh Mahalegi, 2019). It is important to note that, in this isobaric closed homogeneous system, species fractions and temperature results remain consistent regardless of the volume scale, as only gas-phase chemistry is considered in this study, and surface chemistry is not a factor.

Numerical simulations are employed to compute the ignition delay times (IDTs) for the extracted points from the regime diagrams. Specifically, for methane and syngas fuels, the GRI-Mech 3.0 mechanism is used, and for propane fuel, the USC-Mech 2.0 mechanism is utilized. These mechanisms are validated against corresponding experimental data from Ebrahimi Fordoei and Mazaheri (2021), and Yang et al. (2022), ensuring their accuracy in predictions. The individual fuel mechanisms align well with the experimental results, as depicted in Figure 3, justifying their use in the IDT calculations.

The ignition delay times (IDTs) for the selected points from the regime diagrams obtained through numerical simulations are presented in Figure 4 for all the five fuel cases. The plot is segmented into four regions: Regions 1, 2, 3, and 4 correspond to no-combustion, the borderline between MILD and no-combustion, the MILD regime, and the HiTAC combustion regimes, respectively. A significant decrease in ignition delay times (IDTs) is observed while moving from regions 1 to 4, as depicted in Figure 4. It is important to note that the IDTs at the borderline locations (region 2) remain consistent across for all the fuels, maintaining the same range. However, the actual magnitudes vary depending on the specific fuel mixture. This observation underscores that the IDTs remain relatively stable for a given fuel as the flame transitions from a no-combustion to a MILD regime.

Based on the observations from the regime diagrams, IDTs of the MILD regime are primarily influenced by factors such as mixture pressure, temperature, fuel concentrations, oxygen levels, and the presence of other diluents. In this section, the authors specifically studied the IDTs at the boundary between the no-combustion and MILD regimes for the various fuel reactant mixtures. Several important observations are made during this analysis and are:

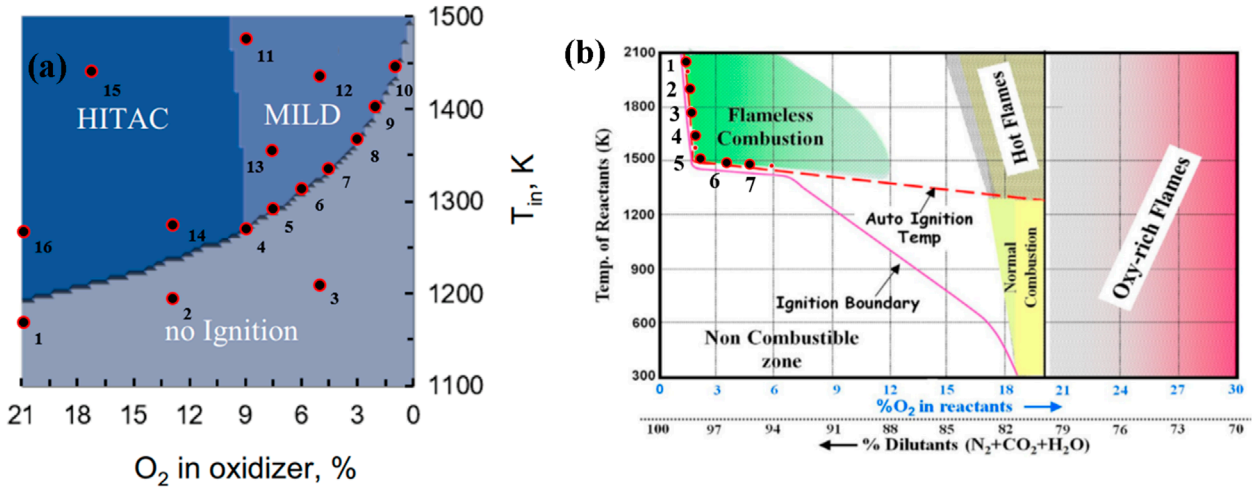

FIGURE 1
Methane combustion regimes diagram under the **(A)** O_2 dilution. Adapted from (Garnayak et al., 2022) with the permission of Taylor & Francis. **(B)** exhaust gas recirculation (Rao and Levy 2010).

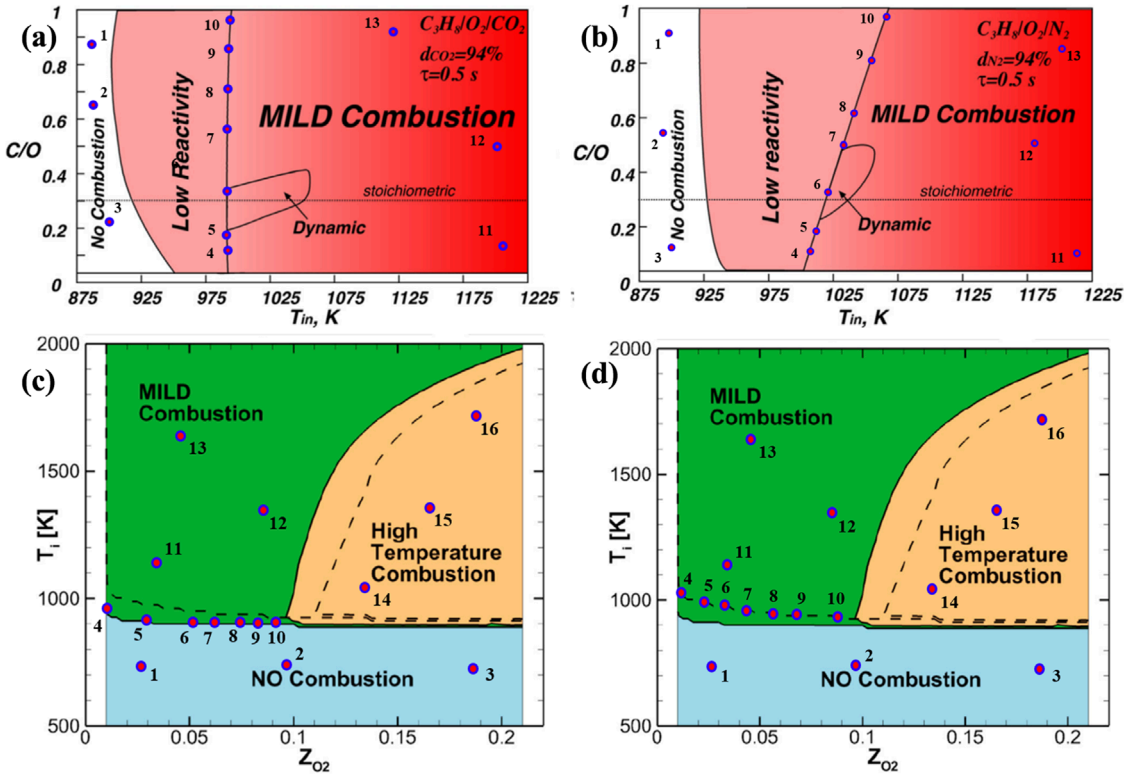

FIGURE 2
Propane combustion regimes diagram for **(A)** H_2O **(B)** N_2 dilutions, Adapted from (Sorrentino et al., 2016) with the permission of Springer and **(C)** syngas (continuous lines), **(D)** enriched syngas (dashed lines) Adapted from (Kim et al., 2021) with the permission of Elsevier.

- The ignition delay times (IDTs) at the examined borderline were consistent in magnitude range for various fuels but varied between different fuel types.
- The magnitudes of the IDTs for various fuels on the considered borderline are followed as C_3H_8/CO_2 > C_3H_8/N_2 > Syngas > CH_4 > Enriched syngas.

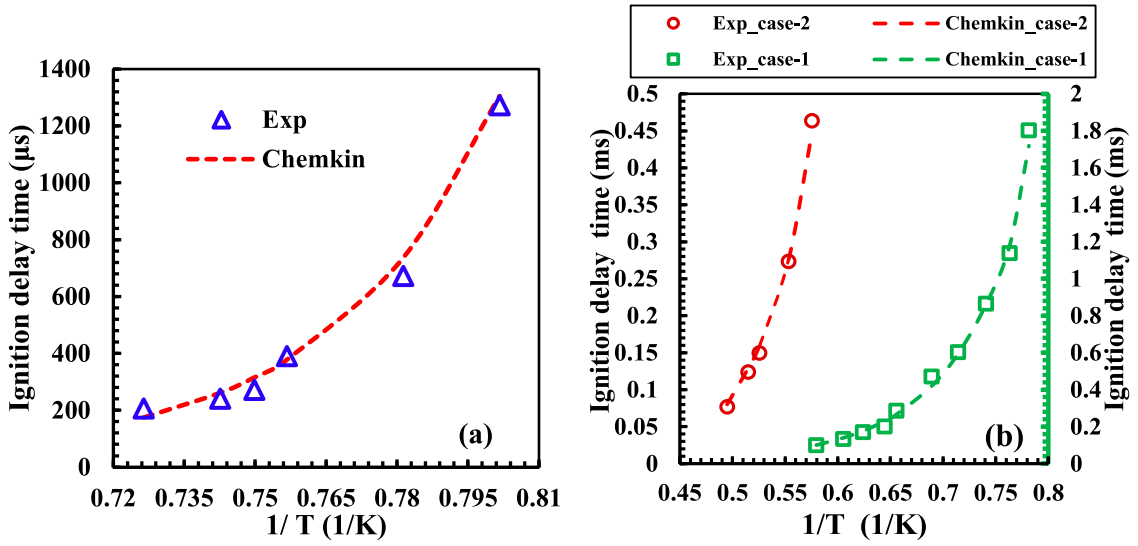

FIGURE 3
Comparison of simulated and experimental IDTs for **(A)** methane and **(B)** propane fuels.

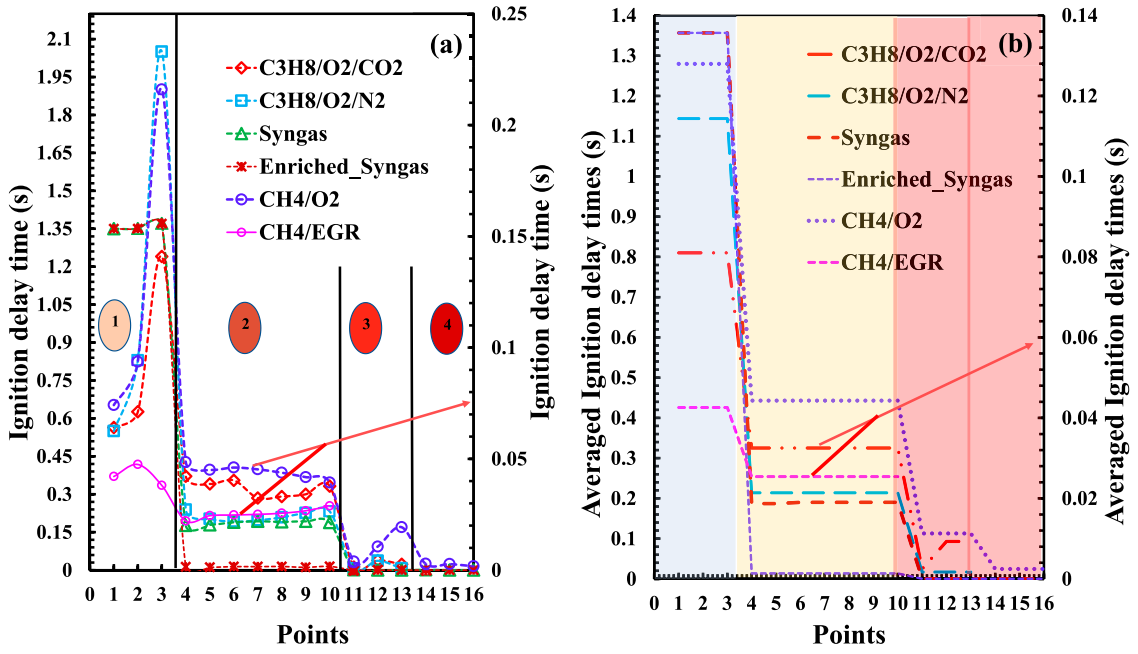

FIGURE 4
(A) Computed IDTs of the extracted data points and **(B)** averaged IDTs in each zone.

3 MILD regime-based analysis for methane fuel

The consistency in the nature of ignition delay times (IDTs) at the borderline points is observed irrespective of the mixture preheating temperature and dilution level in the preceding section. For further in-depth analysis of the borderline points for a given fuel and oxidizer mixtures under various diluted conditions, combustion regime diagrams are not available in the literature. Hence, in this section, multiple combustion regime diagrams for methane fuel are generated using a 1D plug-flow reactor (PFR) within Chemkin Pro. Since the combustion initiation location and peak temperature in the flow are the major factors in determining the stability and regime of the reactant mixture, a Plug Flow Reactor (PFR) is being considered for developing the regime diagram. These diagrams cover different dilutions involving N_2, CO_2, H_2O, and exhaust gas recirculation (EGR) for both with and without H_2 blends as a function of O_2 dilution level and reactant mixture temperatures.

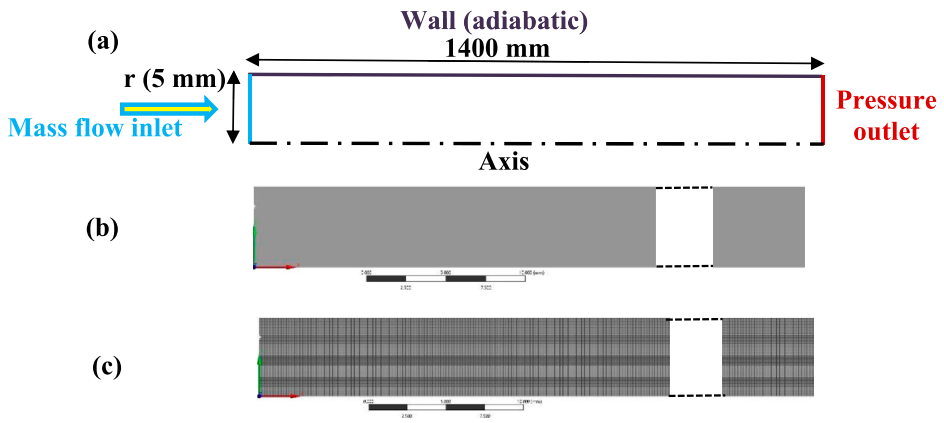

FIGURE 5
Computational domain **(A)** line diagram with boundary conditions **(B)** geometry **(C)** mesh.

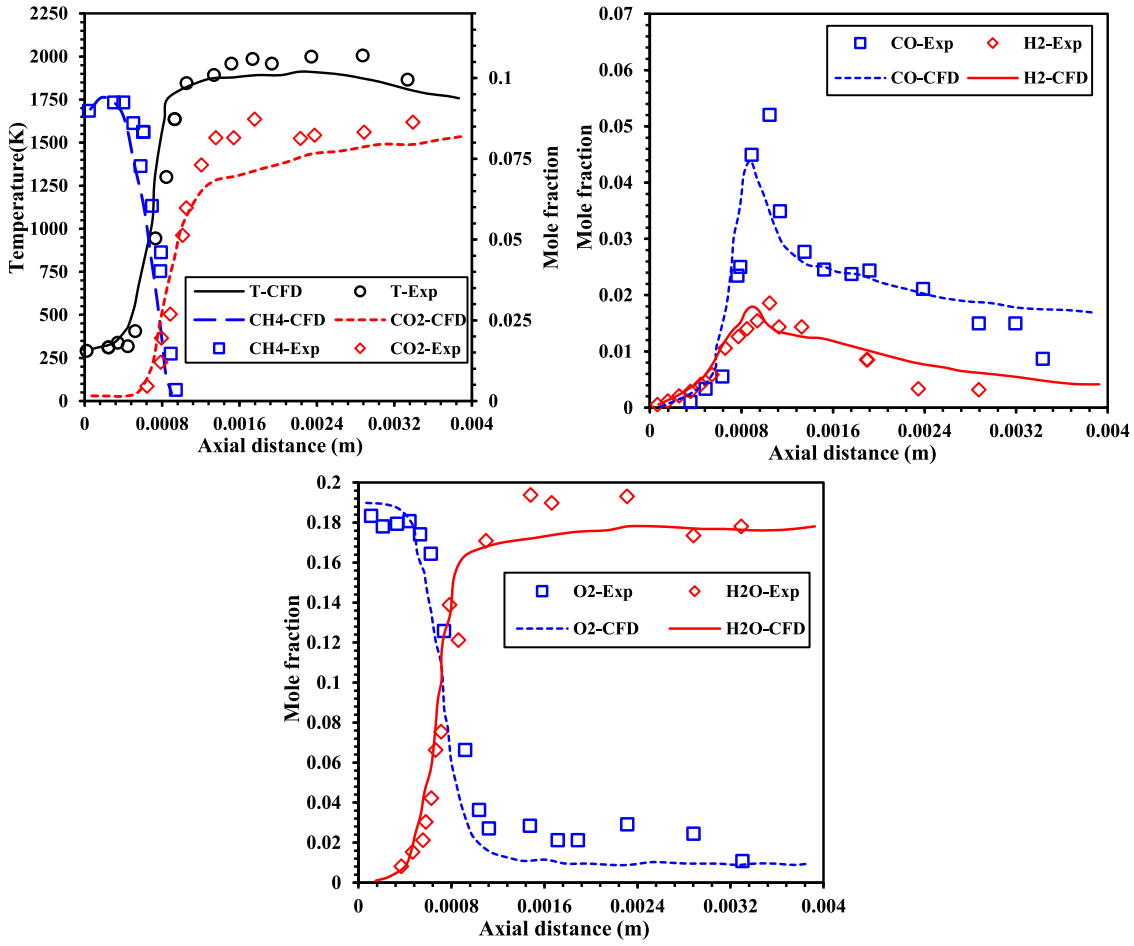

FIGURE 6
Comparison of experimental data with the computational predictions.

3.1 Plug flow reactor (PFR) modeling

The combustion regime diagrams of methane and hydrogen-assisted methane mixtures that are reported in the following sections are developed using an adiabatic plug flow reactor (PFR) module in Chemkin Pro. The numerical simulations are performed under highly preheated and diluted conditions in one-dimensional, steady state, and constant pressure laminar premixed conditions.

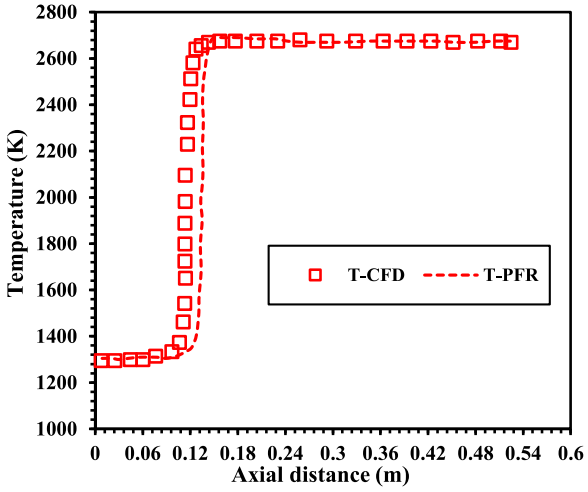

FIGURE 7
Comparison of computational predictions with PFR results.

A well-proved detailed chemical kinetics mechanism of GRI Mech 3.0 is used for conducting the numerical simulations. The plug flow reactor within Chemkin Pro efficiently solves the continuity, momentum, energy, and species first-order ordinary differential equations (ODEs), without considering transport features. This simplification enhances computational efficiency. In this model, the fuel and oxidizer mixture entering the PFR is presumed to be perfectly mixed in the radial direction. The experimental tubular reactor developed by Sabia et al. (2013) is considered for the numerical simulation using PFR. The characteristics of methane mixtures under conditions involving dilution and preheating are assessed within a domain with a 10 mm diameter and a length of 1,400 mm. The methane mixtures are simulated at stoichiometric premixture conditions with N_2, CO_2, H_2O, and EGR by ranging oxygen concentration and preheating temperature of the mixture. The oxygen concentration in the oxidizer is considered from 21% to 0.25% and the inlet reactant preheating temperature is varied from 1100 K to 1700 K. The jet Reynolds number calculated for all the considered cases is approximately 1750. The inlet premixture velocity of 30 m/s is considered as a base case (Garnayak et al., 2022) at a reactant temperature of 1300 K and pressure of 1 atm, and accordingly, the mass flow rate is calculated with 21% oxygen concentration in the oxidizer. The uniform mass flow rate of 0.00061 kg/s is given at the inlet boundary for all the evaluated cases. A similar tubular reactor is also used for developing the combustion regime diagrams by Garnayak et al. (2022).

3.2 CFD modelling and validation

To gain a deeper understanding of the selected flames from the PFR analysis, detailed numerical simulations were conducted using a tubular burner. The burner dimensions match those used in the PFR investigation. The computational domain, along with the finalized grid, comprises 408,051 grid points and 400,000 elements, as illustrated in Figures 5A–C. The radial direction is divided into 50 grids, while the axial direction contains 8,000 grid points. This computational grid is more refined than in previous studies (Garnayak et al., 2022), which employed 240,000 grid points. The boundary conditions applied are also depicted in Figure 5A. All simulations were performed in the OpenFOAM environment, following a methodology consistent with our prior work (Srinivasarao et al., 2023). The earlier study detailed the mathematical modeling and model validation for both pure methane and hydrogen-enriched methane flames.

A direct comparison between the present numerical results and experimental data for identical burner geometries at atmospheric pressure could not be conducted, as such data were unavailable. However, relevant experimental information was found for one-dimensional flame geometries using stoichiometric methane-air mixtures at atmospheric pressure (Bechtel et al., 1981; Stephenson, 1979). In their experiments, Bechtel et al. (1981) employed laser Raman scattering to obtain detailed measurements of temperature profiles and species concentrations in premixed, laminar methane-air flames. Further information about the experimental setup, including the burner configuration, can be found in the studies by Bechtel (1979), Bechtel et al. (1981), and Stephenson (1979).

In this study, the numerical results were evaluated by comparing the centerline temperature and species concentration profiles from the CFD simulations with the experimental data from Bechtel et al. (1981), as illustrated in Figure 6. To ensure consistency, the inlet conditions for the stoichiometric methane-air mixture were set to an initial temperature of 300 K and an inflow velocity of 0.3 m/s. The comparison revealed good agreement between the simulation outcomes and the experimental measurements, validating the accuracy of the numerical approach. The close alignment between the numerical and experimental data confirms that the adopted simulation methodology effectively captures the combustion characteristics under the investigated conditions, demonstrating its reliability for use in this work. Further to see the deviation of the predictions between the CFD and PFR a flame is simulated with methane having mixture temperature of 1300K and 21% O_2 under N_2 diluted condition. Figure 7 shows the axial temperature variation for CFD and PFR. The flame is initiated earlier in case of the CFD as compared with the PFR. The PFR model does not account for key aspects such as mixing phenomena, geometric dependency, and turbulence effects. However, it remains a valuable tool for gaining theoretical insights into the combustion characteristics of various mixtures. In this study, a tubular burner was used, with premixed reactant mixtures supplied uniformly. As a result, the influence of burner geometry and turbulence induced by mixing is minimal. Consequently, the comparison between the axial temperature profiles from the PFR model and CFD simulations shows only slight deviations, validating the applicability of the PFR model under these specific conditions.

3.3 Methane regime diagrams

The regime diagrams are constructed using the PFR modeling approach described in the earlier section. Figures 8A–D represents the methane combustion regime diagrams for N_2, CO_2, H_2O, and EGR as a function of reactant temperature and oxygen concentration in the reactants. In the EGR mixture, 5.5% of CO_2,

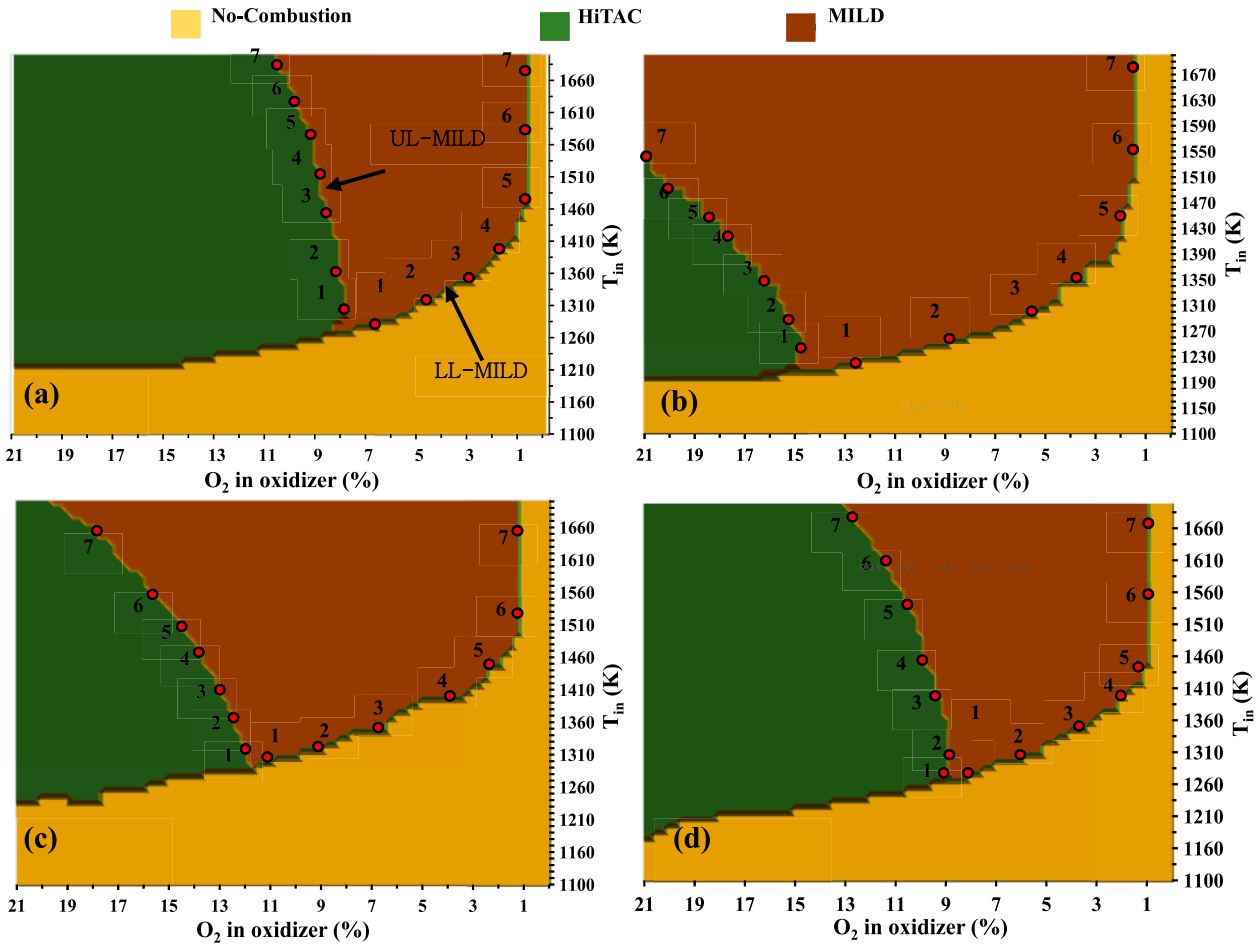

FIGURE 8
Combustion regime diagrams for methane mixtures with **(A)** N_2, **(B)** CO_2, **(C)** H_2O, and **(D)** exhaust gas recirculation (EGR).

6.5% of H_2O, and the remaining adjusted N_2 and O_2 based on the dilution level according to Christo and Dally (2005), Dally, Karpetis and Barlow (2002). Three types of combustion regimes termed no-combustion, HiTAC, and MILD are identified. The combustion regime diagrams are built on the basis of peak temperatures observed in stable reactants temperature profiles within the considered length of the PFR. For the preparation of these regime diagrams, numerous computational simulations are performed with the help of an adiabatic, steady, one-dimensional laminar premixed plug flow reactor (PFR). No-combustion region where the combustion process is not initiated within the considered PFR. A temperature increases lower than 100 K is deemed indicative of an unstable reactant mixture, typically observed as a flame anchored near the exit of the burner. This observation persists even when the mixture temperature exceeds the self-ignition temperature typically associated with flames in the no-combustion regime. This is primarily because the residence time of the unburned mixture entering the PFR (τ_{res}) is shorter than the ignition delay time (τ_{ign}). In situations where the PFR length exceeds its current 1,400 mm, a perfectly stable temperature profile would have been achieved. However, the PFR length is uniform for all the simulated conditions. The boundary that distinguishes the no-combustion and MILD and MILD and HiTAC regimes is roughly within a 10–15 K range on the temperature scale (in T_{in} scale). This small area is not included in the no-ignition zone for basic analysis, nor is it shown in Figure 8. The spread of the no-combustion regime is narrower in the $CH_4/O_2/CO_2$ regime diagram and wider in the $CH_4/O_2/H_2O$ diagram, compared to the other two considered diluted reactant mixtures. This discrepancy can be attributed to the fact that ignition delay times are longer in the case of H_2O-added mixtures when compared to CO_2-added methane mixtures. However, at higher mixture temperatures and lower dilutions (1.5%), a widespread no-combustion region is observed for $CH_4/O_2/CO_2$ mixtures (Figure 8B). Whereas in the $CH_4/O_2/CO_2$ mixtures, the no-combustion regime is limited to 0.5% dilution at higher mixture temperatures (Figure 8A).

In Figures 8A–D, the MILD and HiTAC regimes are defined based on the peak temperatures generated within the considered PFR. It is important to note that the MILD combustion mode is a subset of the HiTAC combustion mode. In the case of MILD combustion, the threshold limit is established using the T_{peak}-T_{mix} weightage, as suggested by Cavaliere and de Joannon (2004). A larger MILD regime is observed in the $CH_4/O_2/CO_2$ mixtures. Conversely, the $CH_4/O_2/N_2$ mixtures exhibit a narrower MILD regime. In the overall, CO_2, H_2O, and EGR-assisted

TABLE 1 Collected borderline points for methane mixtures.

Point number	$CH_4/O_2/N_2$				$CH_4/O_2/CO_2$			
	LL-MILD		UL-MILD		LL-MILD		UL-MILD	
	Tin (K)	O_2 (%)	Tin (K)	O_2 (%)	Tin (K)	O_2 (%)	Tin (K)	O_2 (%)
1	1,280	6.75	1,300	7.75	1,220	12.5	1,220	14.75
2	1,320	4.5	1,370	8	1,250	9	1,280	15.25
3	1,350	3	1,450	8.5	1,300	5.5	1,350	16.25
4	1,400	1.75	1,520	8.75	1,350	3.5	1,400	17.25
5	1,470	0.75	1,580	9.25	1,450	1.75	1,450	18.5
6	1,580	0.75	1,620	9.75	1,550	1.5	1,500	20.25
7	1,680	1	1,680	10.5	1,680	1.5	1,550	21
	$CH_4/O_2/H_2O$				$CH_4/O_2/EGR$			
1	1,300	11	1,320	11.75	1,270	8.25	1,270	9
2	1,320	9	1,370	12.25	1,300	6	1,300	8.5
3	1,350	6.5	1,420	13	1,350	3.5	1,400	9.25
4	1,400	3.5	1,470	13.75	1,380	2.25	1,470	9.75
5	1,450	2	1,520	14.5	1,420	1.25	1,550	10.75
6	1,520	1.25	1,570	15.75	1,550	1	1,600	11.25
7	1,650	1.25	1,650	17.75	1,670	1	1,670	12.5

Tin: Reactant inlet mixture temperatures.
LL-MILD: Borderline between no-combustion and MILD.
UL-MILD: Borderline between MILD and HiTAC.

methane mixtures have a broader operating range under the MILD combustion mode. Building upon the intriguing observations made in the previous section, the analysis focused on the borderlines between the no-combustion and MILD and MILD and HiTAC combustion regimes. On these borderlines, seven points for the analysis are selected, as depicted in Figures 8A–D. The data points extracted for the methane combustion regime diagrams presented in Figures 8A–D are compiled in Table 1 for further examination.

The Ignition Delay Times (IDTs) for the selected borderline points are calculated through numerical simulations employing a 0D closed homogeneous reactor with the GRI Mech 3.0 mechanism. From the perspective of IDTs for the analysis purpose, the borderline between the no-combustion and MILD regimes represents the lower limit of the MILD regime (LL-MILD), while the borderline between the MILD and HiTAC regimes marks the upper limit of the MILD regime (UL-MILD).

Figures 9A–D shows the calculated ignition delay times (IDTs) for the various methane mixture scenarios. These IDTs are derived from the seven selected points, sequentially labelled one to seven, and represent how the IDTs are changing as a function of mixture temperature and oxygen dilution levels. The LL-MILD line signifies the boundary separating the no-combustion and MILD regimes, while UL-MILD marks the borderline between the MILD and HiTAC regimes. The UL-MILD IDTs for all methane mixture cases showed linear variation as the mixture temperatures increased along with a reduction in oxygen concentrations. Whereas UL-MILD IDTs showed consistent behaviour till the 5th point, where the inlet temperature (T_{in}) is less than or equal to 1500 K. This consistency underscores that the IDTs are uniform and stable in this specific temperature and oxygen concentration range for all methane mixtures studied in Figures 9A–D. On the other hand, the increase in the mixture temperatures is compensated by the reduction in the oxygen concentrations in the reactant mixture. This individual effect, especially from the oxygen concentration, is further detailed in the next sections.

The variation in the no-combustion regime remains constant once the reactants' temperature reaches 1500 K. In other words, with further reduction in the oxygen concentrations in the mixture at a given 1500 K reactant temperatures, the reactants are not burned within the considered PFR. However, a significant and abrupt change in ignition delay time is observed for points beyond a mixture temperature of 1500 K, as the reactant temperature is

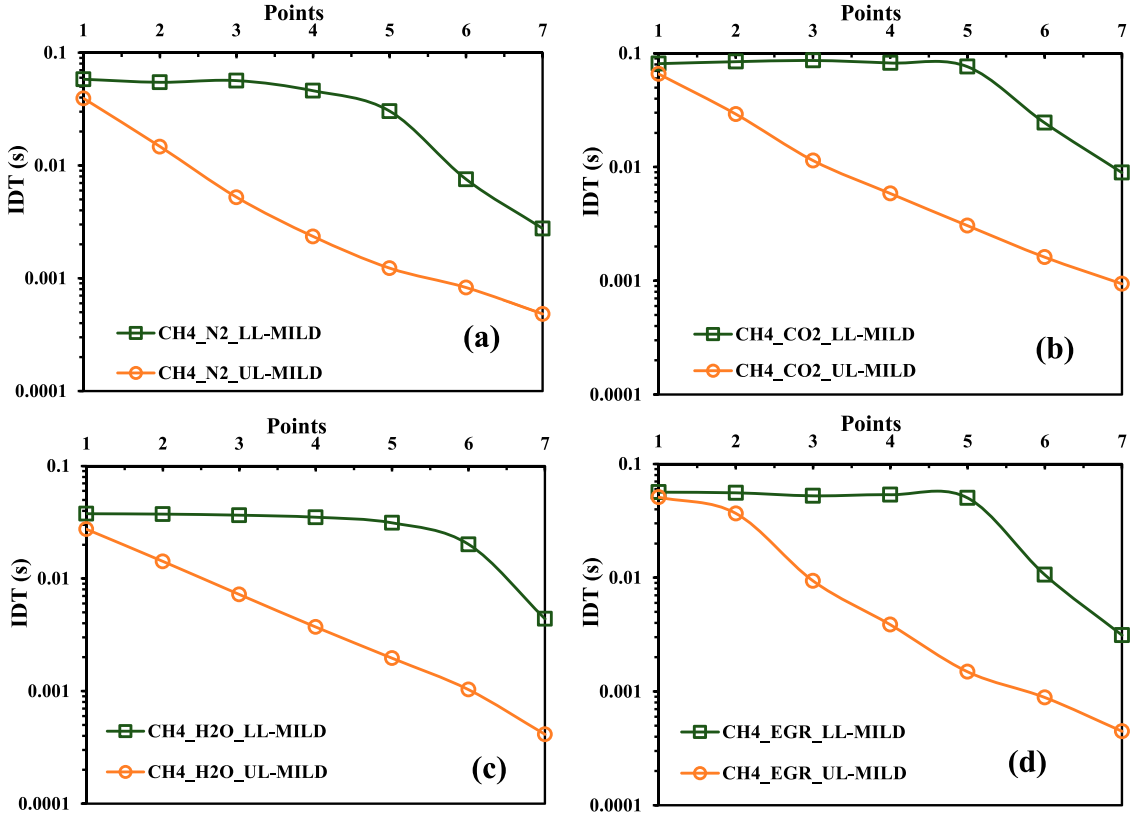

FIGURE 9
Ignition delay times for the collected points on the borderlines for methane mixtures with **(A)** N_2, **(B)** CO_2, **(C)** H_2O, and **(D)** exhaust gas recirculation (EGR).

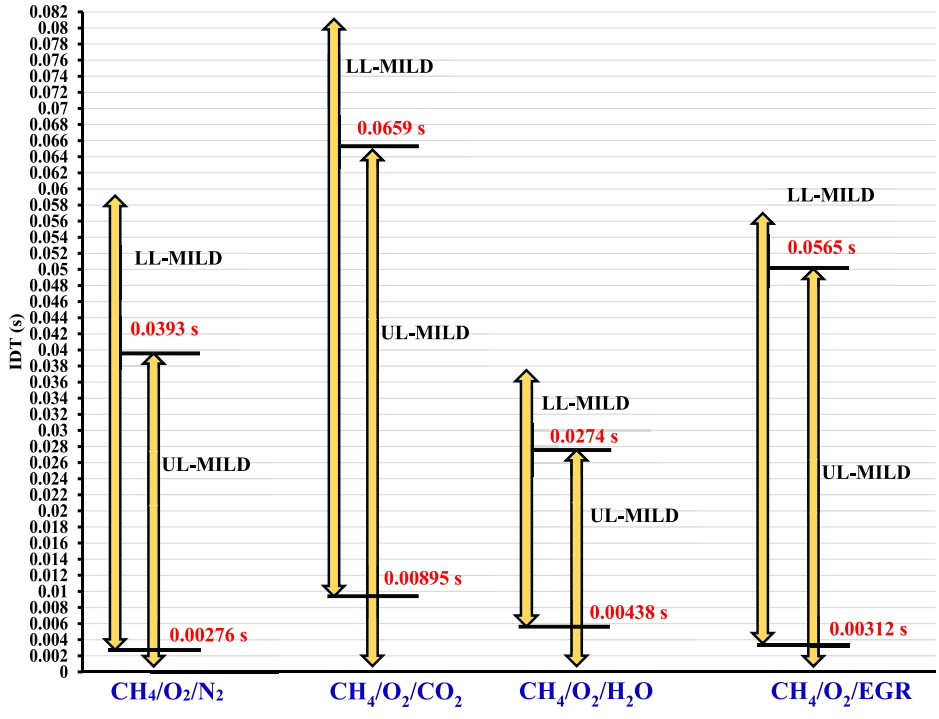

FIGURE 10
Minimum to maximum ranges of IDTs on LL-MILD and UL-MILD for the methane mixtures.

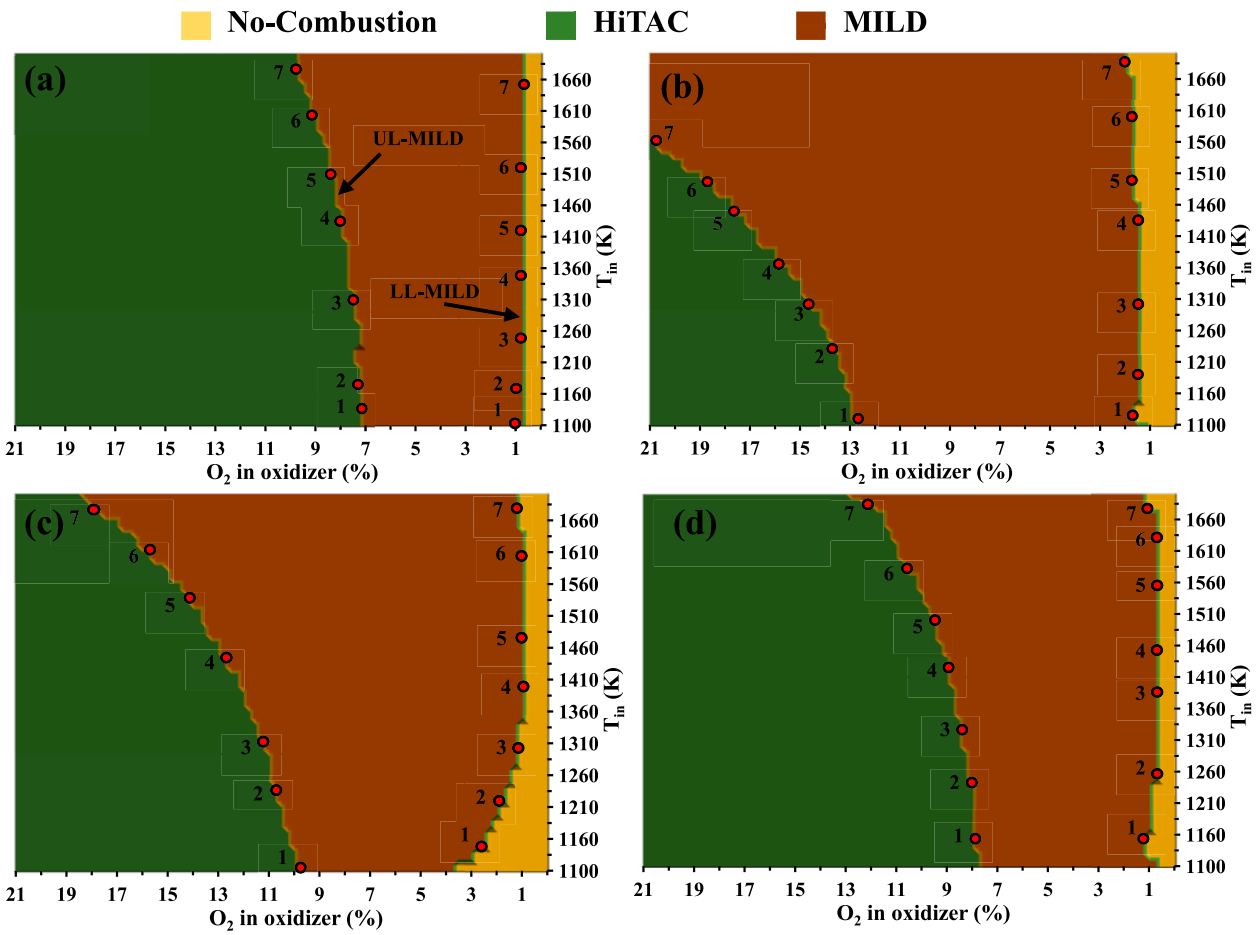

FIGURE 11
Combustion regime diagrams for hydrogen-assisted methane mixtures with **(A)** N_2, **(B)** CO_2, **(C)** H_2O, and **(D)** exhaust gas recirculation (EGR).

further increased at a constant O_2 (points 6 and 7). On the other hand, at a fixed mixture temperature of 1500 K, the upper limit of the burned gas temperature in the MILD regime is approximately 2373 K. It is a well-established fact that, for hydrocarbon fuels, flame temperatures should be controlled within the range of 1900 K to reduce the emissions (Wünning and Wünning, 1997). Therefore, an analysis is made from an emissions perspective to gain a deeper understanding of MILD combustion characteristics, focusing on CO and NO emissions. This will be discussed in the next section of the present work. Notably, it is important to highlight that the UL-MILD IDTs do not exhibit a similar magnitude trend when compared to the LL-MILD IDTs. The difference in height between the LL-MILD and UL-MILD plots within a specific case serves as an indicator of the broad range of IDT magnitudes characterizing the MILD regime. For a given mixture temperature and O_2 concentration in the mixture, the IDTs for $CH_4/O_2/CO_2$ mixtures are lower than those for $CH_4/O_2/H_2O$ mixtures. However, the trend is reversed for LL-MILD ($\tau_{CH4/O2/CO2} > \tau_{CH4/O2/H2O}$). This difference can be attributed to the temperature difference (T_{peak} - T_{mix}) between the no-combustion regime and the MILD regime. In the case of $CH_4/O_2/CO_2$ mixtures, this temperature difference is around 120 K, whereas, for $CH_4/O_2/H_2O$ mixtures, it is approximately 400 K when transitioning from the no-combustion regime to the MILD regime. This temperature difference accounts for the reduction in IDT for $CH_4/O_2/H_2O$ mixtures in the LL-MILD scenario. On the other hand, CH_4/O_2/EGR mixtures exhibit an intermediate behaviour between $CH_4/O_2/H_2O$, and $CH_4/O_2/CO_2$ mixtures. The chemical effect of H_2O and CO_2 on the MILD combustion behaviour also explained in Mardani et al., 2013; Sabia et al., 2016.

Figure 10 shows the minimum and maximum ignition delay times (IDTs) observed in each scenario for LL-MILD and UL-MILD of methane regime diagrams. These IDTs play a crucial role in determining the optimal range for operating the MILD combustion. When an IDT exceeds the range identified as overlapping, it indicates no combustion. Conversely, if the IDT falls below the overlapping range, the mixture is more effective at generating high-temperature regions.

3.4 Hydrogen-assisted methane regime diagrams

In a manner similar to the methane combustion regime diagrams, combustion regime diagrams for hydrogen-assisted

10.3389/fenrg.2024.1503787

TABLE 2 Collected borderline points.

Point number	CH_4-H_2/O_2/N_2				CH_4-H_2/O_2/CO_2			
	LL-MILD		UL-MILD		LL-MILD		UL-MILD	
	Tin (K)	O_2 (%)	Tin (K)	O_2 (%)	Tin (K)	O_2 (%)	Tin (K)	O_2 (%)
1	1,100	1	1,130	7	1,120	1.75	1,120	12.75
2	1,170	1	1,250	7.25	1,170	1.5	1,230	13.5
3	1,250	0.75	1,350	7.5	1,300	1.5	1,300	14.5
4	1,350	0.75	1,450	8	1,430	1.5	1,370	15.75
5	1,420	0.75	1,550	8.5	1,500	1.75	1,450	17.5
6	1,520	0.75	1,600	9	1,600	1.75	1,500	18.75
7	1,650	0.75	1,670	9.75	1,690	2	1,550	20.5
CH_4-H_2/O_2/H_2O					CH_4-H_2/O_2/EGR			
1	1,150	2.5	1,100	9.75	1,170	1	1,150	7.75
2	1,220	1.75	1,220	10.5	1,250	0.75	1,250	8
3	1,300	1.25	1,320	11.25	1,380	0.75	1,330	8.25
4	1,400	1	1,430	12.5	1,450	1	1,420	8.75
5	1,480	1	1,530	14	1,550	1	1,500	9.5
6	1,600	1	1,600	15.5	1,630	1	1,580	10.5
7	1,680	1.25	1,670	17.5	1,670	0.75	1,670	11.25

Tin: Reactant inlet mixture temperatures.

methane combustion are developed, incorporating N_2, H_2O, CO_2, and EGR under highly preheated and diluted conditions, as illustrated in Figures 11A–D. For the computational simulations, methane and hydrogen are supplied in equal volumes in the fuel stream. The analysis for the hydrogen-assisted methane flame, including LL-MILD and UL-MILD points, follows a similar approach to the methane regime diagrams.

The introduction of hydrogen into the methane flame across all scenarios leads to a significant reduction in the no-combustion region. This phenomenon can be attributed to the addition of highly flammable hydrogen, which extends the flammability range of the unburned mixture and subsequently results in shorter ignition delay times for the same volumetric flow rate. Among the four considered cases, the no-combustion region (O_2 of 0.75%) is notably minimized in the CH_4-H_2/O_2/N_2 mixtures, as depicted in Figure 11A. In contrast, a larger no-combustion region is evident in the CH_4-H_2/O_2/CO_2 mixtures. This approach of enhancing or controlling flame combustion characteristics by introducing one fuel into another is referred to as fuel blending. While numerous studies have explored the blending of hydrogen into methane combustion, an in-depth examination of the MILD combustion operating range with hydrogen addition to methane mixtures through combustion regime diagrams is lacking in the existing literature. The current study aims to fill this gap by providing valuable insights into the feasibility of achieving MILD combustion through various techniques under atmospheric pressure. It is observed that the introduction of hydrogen into methane mixtures enhances the spread of the MILD combustion region for all the cases depicted in Figures 11A–D, except for CH_4-H_2/O_2/N_2 mixtures. Particularly noteworthy is the stabilization of MILD flames at lower mixture temperatures, which holds significant advantages from an application standpoint. Among the CH_4-H_2/O_2/CO_2, CH_4-H_2/O_2/H_2O, and CH_4-H_2/O_2/EGR mixtures, it is observed that the CH_4-H_2/O_2/CO_2 mixture exhibits a well-controlled effect on the peak temperature generated in the considered PFR. To gain a deeper understanding of the boundaries within the hydrogen-methane mixtures, the LL-MILD and UL-MILD points have been collected and are presented in Table 2.

Following the established methodology used in prior cases, the ignition delay times (IDTs) for the extracted data points have been calculated. The resulting trends in IDT variations are visually depicted in Figures 12A–D for LL-MILD and UL-MILD in each of the considered scenarios. The consistency in the vertical distance separating the LL-MILD and UL-MILD regions holds true across a spectrum of mixture temperatures and various dilution levels. This consistent pattern provides valuable insights into the linear IDT

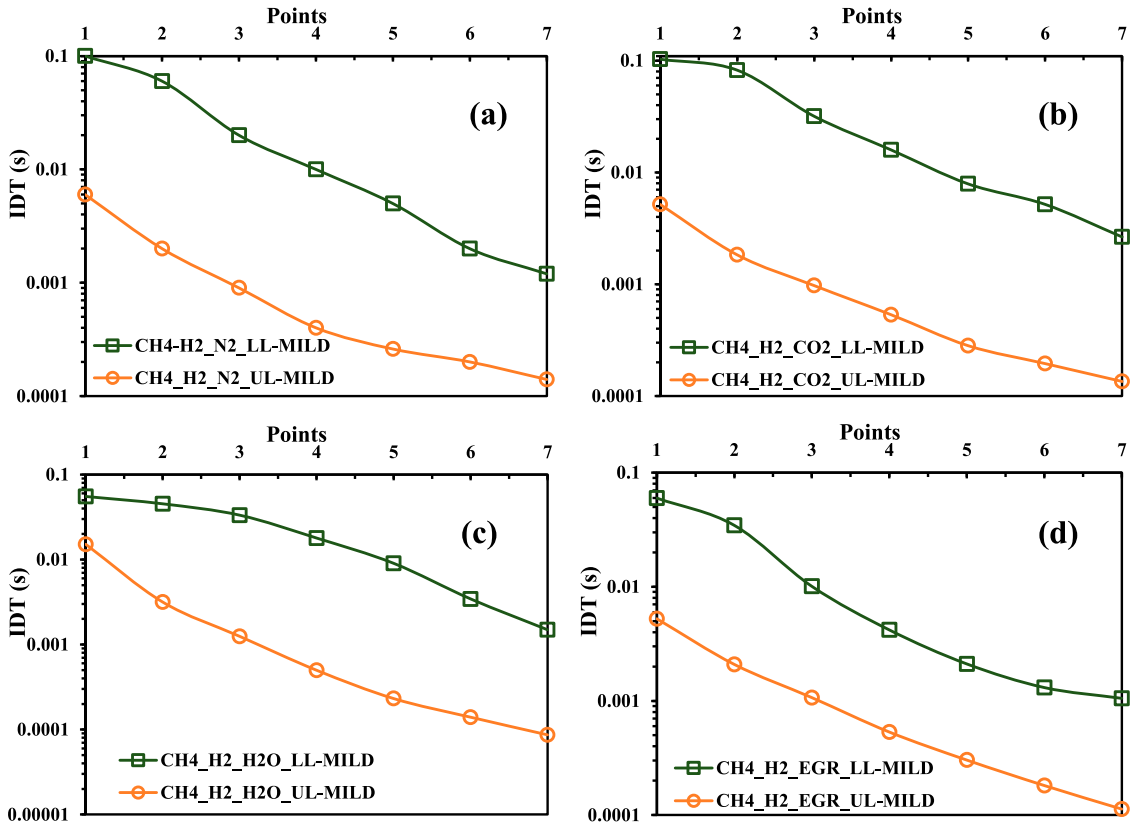

FIGURE 12
Ignition delay times for the collected points on the borderlines for hydrogen-assisted methane mixtures with **(A)** N_2, **(B)** CO_2, **(C)** H_2O, and **(D)** exhaust gas recirculation (EGR).

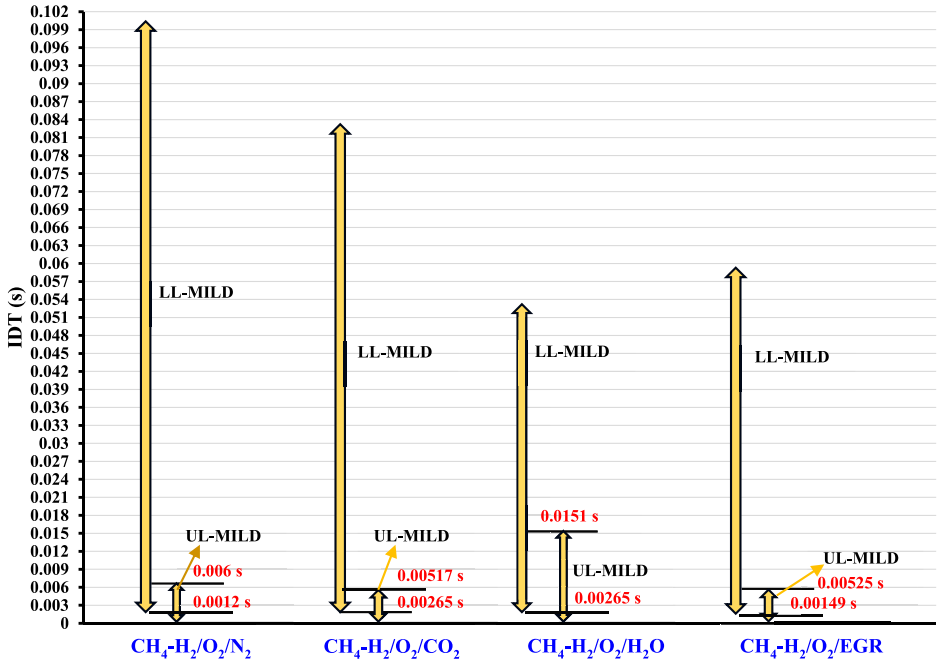

FIGURE 13
Minimum to maximum ranges of IDTs on LL-MILD and UL-MILD for the methane-hydrogen mixtures.

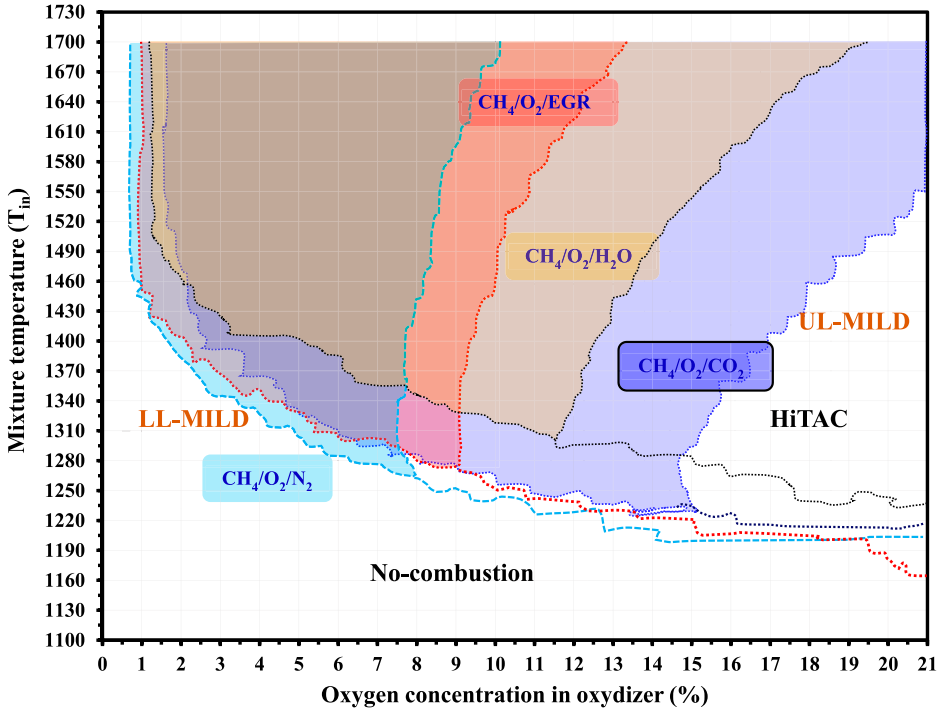

FIGURE 14
Comparison of the MILD regimes of methane flames.

behavior of the hydrogen-methane mixtures with an increase in mixture temperatures and a reduction in oxygen concentrations.

Figure 13 provides a visual insight into the ignition delay times (IDTs) across the various scenarios considered. This overlap in IDTs holds significant implications, particularly for methane-hydrogen mixtures for UL-MILD, as it indicates the presence of a consistent operational range except for CH_4-$H_2/O_2/H_2O$ mixtures. Within this range, the flames exhibit enhanced stability in the MILD combustion regime, allowing for precise control over the maximum flame temperature, a crucial factor in optimizing combustion processes.

3.5 Factor of influence of O_2 dilution level on MILD combustion

The analysis delves into the influence of oxygen concentration on MILD combustion characteristics, considering the presence of N_2, CO_2, H_2O, and EGR over a range of preheating temperatures. To facilitate this investigation, data from the MILD regime extracted from each of the developed combustion diagrams are incorporated into a single plot. The extent of the MILD regime follows a specific order: $CH_4/O_2/CO_2 > CH_4/O_2/H_2O > CH_4/O_2/EGR > CH_4/O_2/N_2$. Significantly, the minimum O_2 concentration required to initiate combustion is observed in the following order at equivalent mixture temperatures: $CH_4/O_2/CO_2$ (1.5%) > $CH_4/O_2/H_2O$ (1.25%) > $CH_4/O_2/EGR$ (1%) > $CH_4/O_2/N_2$ (0.75%). The reactivity of the fuel mixture is strongly influenced by the diluent conditions. For N_2-diluted cases, the minimum oxygen concentration required for flame initiation is the lowest, owing to nitrogen's low specific heat capacity compared to other diluents. This trend follows the specific heat capacity of the diluent: the lower the heat capacity, the less oxygen is needed for flame initiation. In contrast, for H_2O dilution, although water has a high specific heat capacity, it contributes to an OH radical pool, which aids in flame stabilization. As a result, despite its higher heat capacity, H_2O dilution requires less oxygen for flame initiation than other diluents with lower radical generation. Thus, the above order of minimum oxygen requirement for flame initiation is observed. This order reflects the balance between the thermal effect of the diluents and their chemical role in radical formation and flame stabilization. To quantify the impact of O_2 concentration on combustion characteristics concerning changes in mixture temperature, the authors considered the gradient of UL-MILD (dT/dO_2). In essence, to measure the effect of O_2 by measuring how the reduction in O_2 dilution was compensated by the increase in mixture temperature at the UL-MILD borderline. Figure 14 reveals that the gradient or slope of the UL-MILD line signifies the oxygen concentration sensitivity. For the $CH_4/O_2/N_2$ regime diagram, altering the O_2 concentration from 7.75% to 10.5% (a difference of 2.75%) resulted in a shift in mixture temperature from 1270 K to 1700 K (a difference of 430 K) for maintaining the flame within the MILD regime. The average gradient along the UL-MILD borderline of the $CH_4/O_2/N_2$ regime diagram is 156 K. Similarly, the gradients along the UL-MILD borderlines for the $CH_4/O_2/CO_2$, $CH_4/O_2/H_2O$, and $CH_4/O_2/EGR$ regime diagrams are 54 K, 51 K, and 143 K, respectively. A larger gradient signifies a stronger influence of O_2 on the respective fuel mixture. The impact of O_2 is notably higher and consistent for the $CH_4/O_2/N_2$ and $CH_4/O_2/EGR$ flames at higher mixture temperatures (above 1300 K), while it is lower and relatively similar for both $CH_4/O_2/CO_2$ and $CH_4/O_2/H_2O$

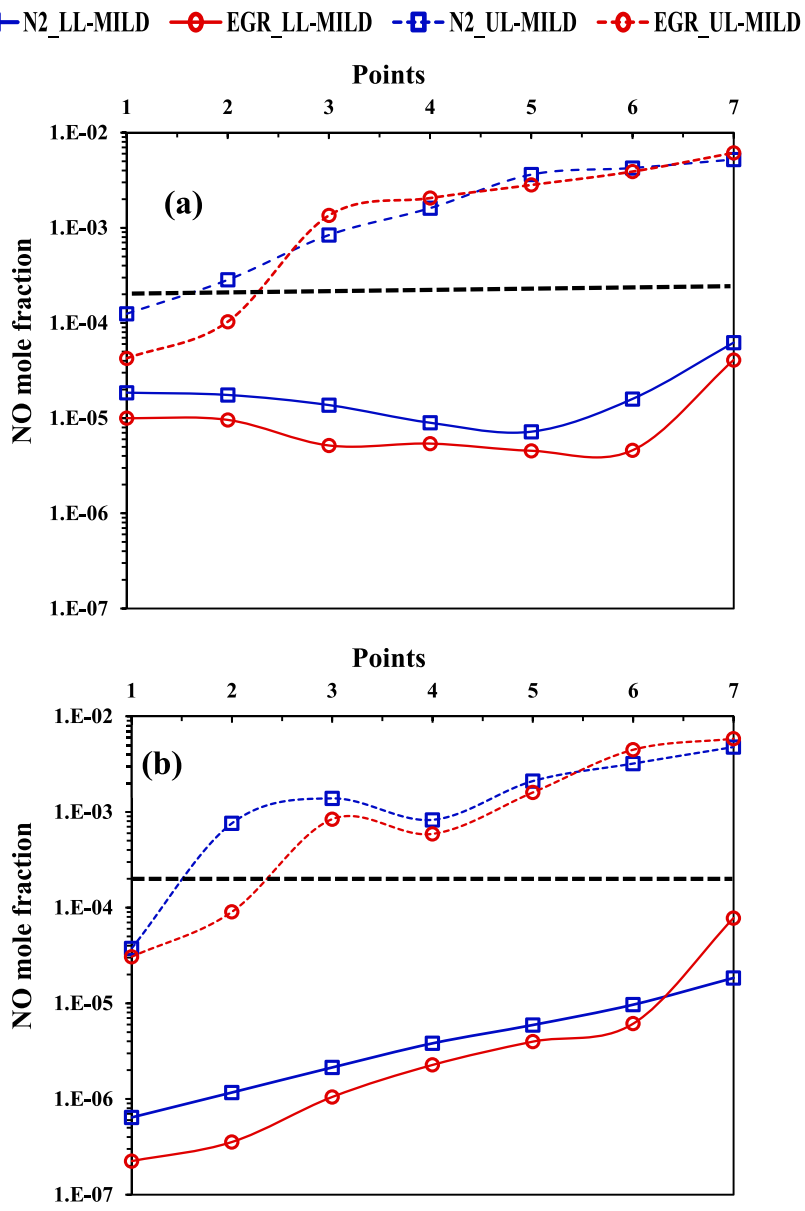

FIGURE 15
Mole fraction of NO at LL-MILD and UL-MILD of the **(A)** methane and **(B)** methane-hydrogen combustion regime diagrams.

mixtures. In all the examined cases of methane mixtures, stable MILD combustion flames are observed, with mixture temperatures ranging from 1450 K to 1700 K and oxygen dilution percentages between 2.5% and 7.5%. A similar kind of behavior is observed for the methane-hydrogen mixtures.

3.6 Emission-based analysis

3.6.1 Analysis of NO emissions

The regime diagrams developed under the influence of CO_2 and H_2O do not contain NO, as these mixtures do not contain the N radical. Consequently, NO levels in the LL-MILD and UL-MILD borders of methane and methane-hydrogen regime diagrams with N_2 and EGR are analyzed in Figure 15. The black horizontal dashed line in Figure 15 represents the upper limit of NO emissions for the MILD regime (lower limit of the IDT), as mentioned in the previous section regarding the overlapping region (Figures 10, 13). Notably, NO production in the MILD regime is observed after the mixture temperature exceeds 1500 K. Therefore, while achieving MILD combustion is possible at higher mixture temperatures, it is advisable to limit preheating temperatures to around or lower than 1300 K to control NO production from the methane flames. The NO emissions are primarily attributed to the elevated temperatures within the burner for higher mixture temperature cases. The NO levels in the overlapping IDT region are nearly identical for both methane and hydrogen-assisted methane mixtures in both EGR and N_2 cases. The mechanism of NOx formation under MILD combustion conditions has been extensively reported in the literature (Iavarone and Parente, 2020; Mardani and Tabejamaat, 2012).

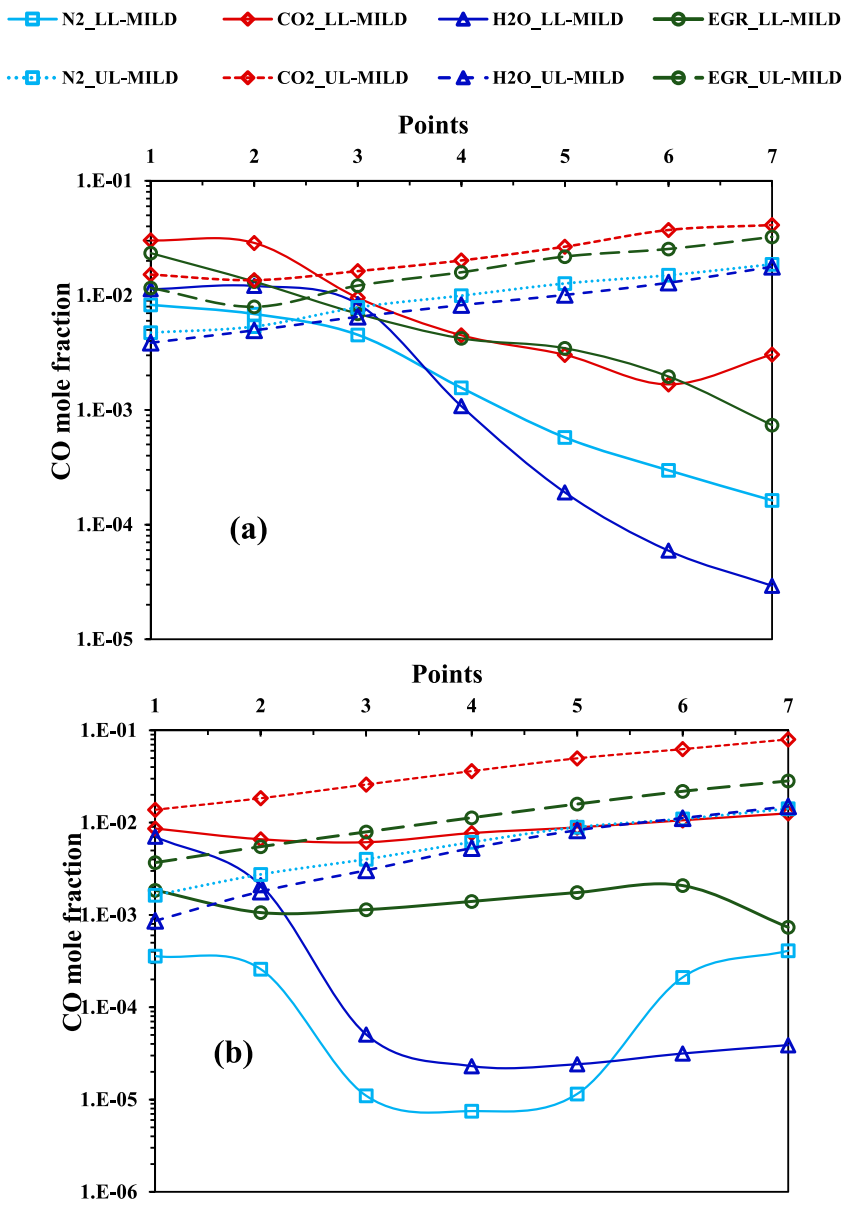

FIGURE 16
Mole fraction of CO at LL-MILD and UL-MILD of the **(A)** methane and **(B)** methane-hydrogen (right side) combustion regime diagrams.

3.6.2 Analysis of CO emissions

Figure 16 illustrates the CO variation at the LL-MILD and UL-MILD borders for both methane and hydrogen-assisted methane flames under the influence of N_2, CO_2, H_2O, and EGR. The UL-MILD border points for both methane and hydrogen-assisted methane combustion regimes exhibit a linear variation along the border (points from 1 to 7) in all the considered cases. In the methane regime diagram, the LL-MILD border points show a reduction in CO emissions with increasing mixture temperature. However, this trend is altered for the UL-MILD border points (Figure 16A). CO emissions are slightly higher in the case of hydrogen-assisted methane flames with CO_2 influence under highly diluted conditions. On the other hand, CO emissions are lower with the hydrogen-assisted methane flames. Similar to NO emissions, CO emissions are more significant at higher mixture temperatures.

3.7 Overall flame behavior

This section analyzes the flame behavior at the lowest and highest points within the LL-MILD (Lower Limit MILD) and UL-MILD (Upper Limit MILD) regimes for all the considered cases. The goal is to examine how the flame front behaves at these extreme points on the lower and upper boundaries of the combustion regimes.

Figure 17 presents the temperature distributions for the first and last selected data points along the upper and lower MILD boundary lines. Flames LL1 and UL1 show moderate peak temperatures,

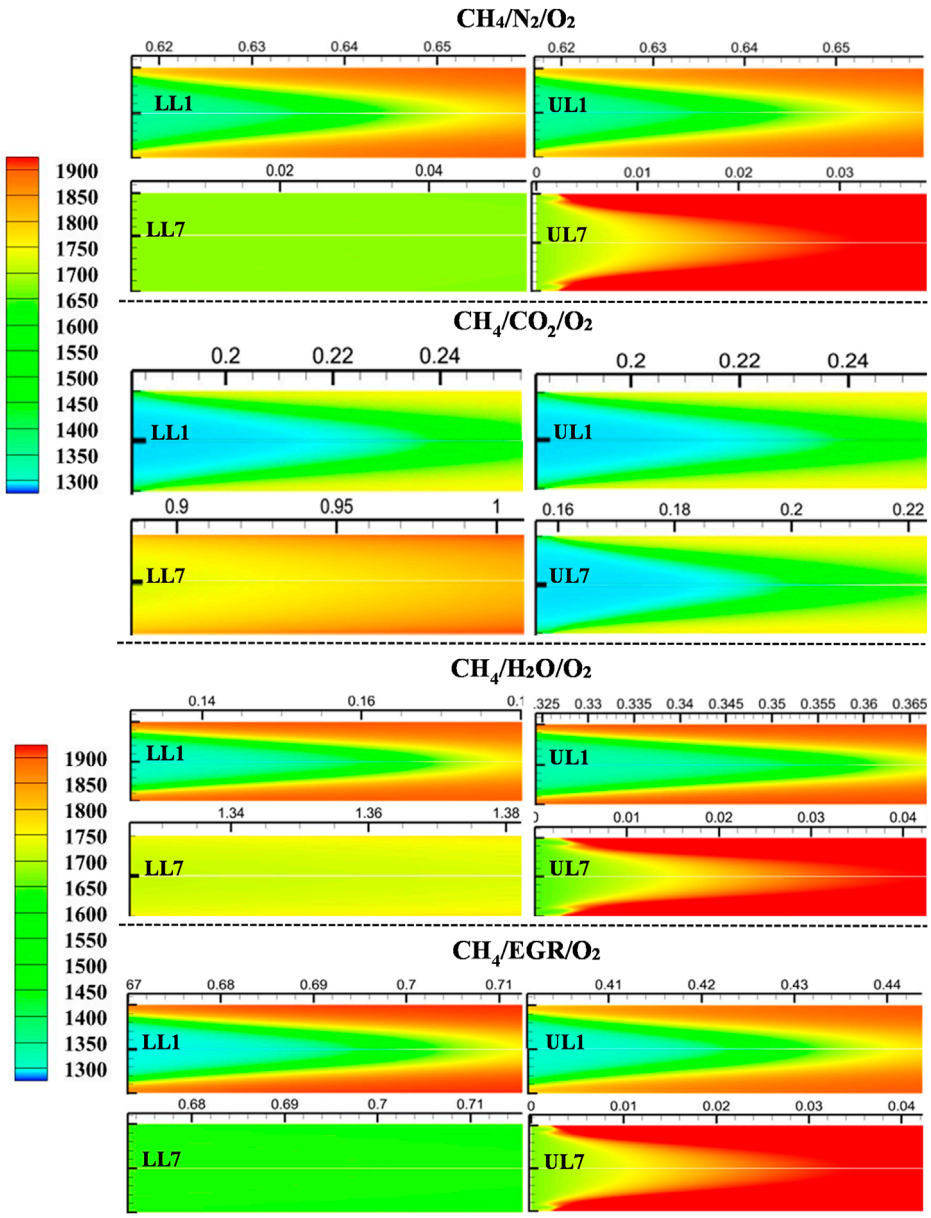

FIGURE 17
Temperature distribution at the flame initiating point for methane mixtures with all the diluted conditions. Here, LL1, LL2, UL1, and UL2 are given as per the tabulated selected mixture from the lower limit and upper limit of the MILD regimes.

with the mixture temperatures ranging between 1,100 and 1300 K. Consequently, the peak temperatures remain below 1800 K, which helps reduce NO emissions. Additionally, the oxygen concentration lies between 7% and 15%, further limiting NO formation by suppressing HNO production. In the case of LL7, the mixture temperature rises to around 1,600–1700 K, but the oxygen concentration drops to below 1.5%. Due to this limited oxygen availability at high temperatures, the observed temperature difference (ΔT) is within 200 K, resulting in a well-distributed temperature profile. On the other hand, in UL7, the mixture temperatures are similar to those in LL7, but the oxygen concentration exceeds 10%. As a result, peak temperatures reach nearly 2200 K. Although these conditions still fall within the MILD regime based on the ΔT criterion, the elevated temperatures lead to significantly higher thermal NOx formation compared to other flames. These trends remain consistent across all diluted cases shown in Figure 17. Among the diluted flames, those with CO_2 dilution show the smallest increase in temperature compared to other diluents. However, across all cases, no localized temperature peaks are observed once the flame stabilizes, confirming the MILD flame characteristics.

Based on these observations and the findings discussed in earlier sections, it is recommended to maintain the ignition delay time within the range defined between LL7 and UL1. This range corresponds to the overlapping ignition delay times identified in previous sections, ensuring stable operation within the MILD regime with low emissions.

Similarly, hydrogen-blended methane mixtures were analyzed under various dilution conditions. Figure 18 illustrates the

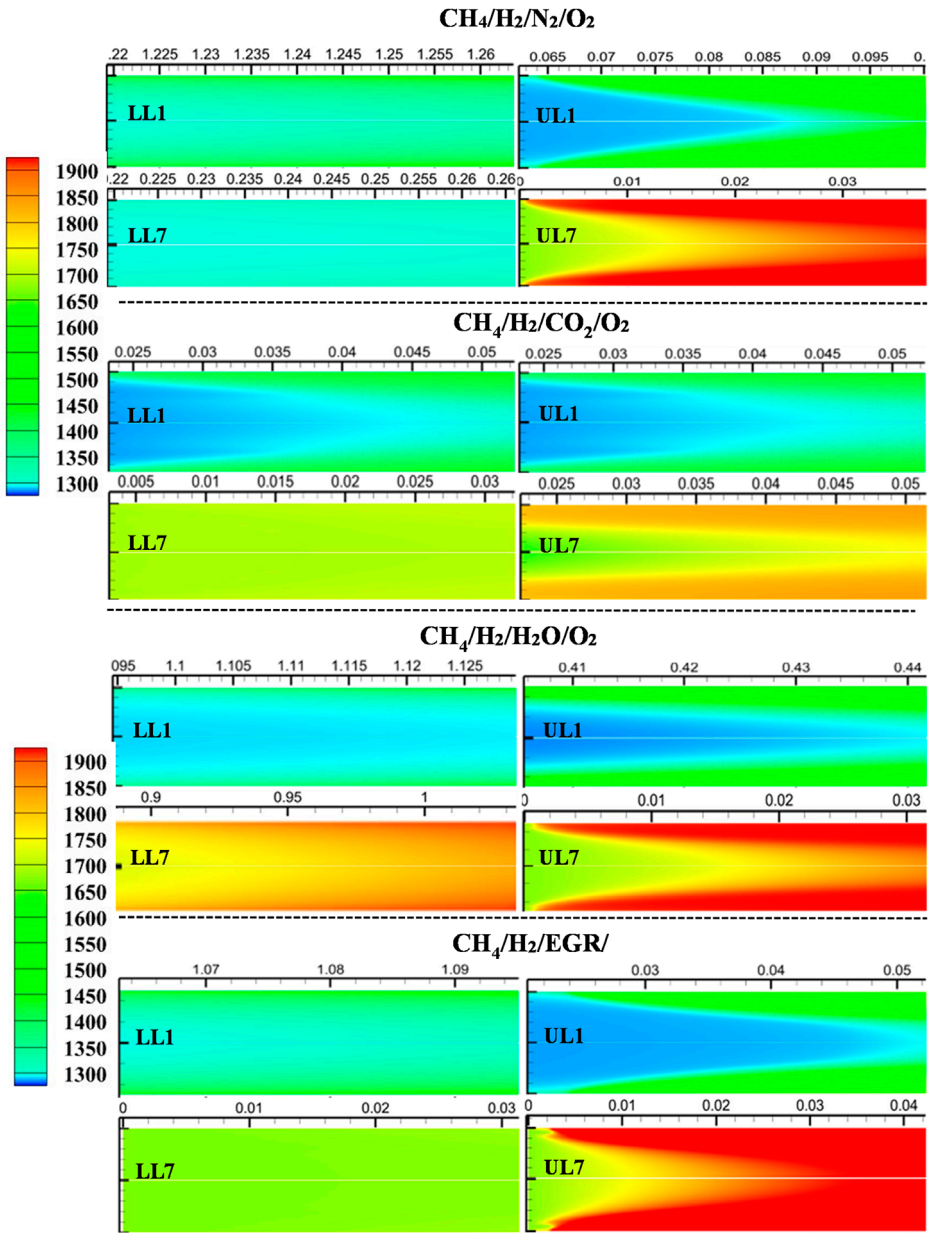

FIGURE 18
Temperature distribution at the flame initiating point for methane-hydrogen mixtures with all the diluted conditions. Here, LL1, LL2, UL1, and UL2 are given as per the tabulated selected mixture from the lower limit and upper limit of the MILD regimes.

TABLE 3 Proposed ignition delay time ranges for achieving MILD combustion regime with lower emissions.

Point number	Methane				Methane-hydrogen			
	N_2	CO_2	H_2O	EGR	N_2	CO_2	H_2O	EGR
Lower limit (ms)	2.7	8.9	4.38	3.1	1.2	2.6	2.6	5.2
Higher limit (ms)	39.3	65.9	27.4	56.5	6.0	5.2	15.1	1.4

temperature distributions for the first and last selected data points along the upper and lower MILD boundary lines in the methane-hydrogen mixture regime diagrams.

The addition of hydrogen led to a decrease in the rise of peak temperatures across all cases. This reduction in temperature increments within the domain further contributed to lower NO emissions, as peak temperatures play a critical role in NO formation. Furthermore, hydrogen addition led to earlier flame initiation for the respective diluted cases, enhancing ignition stability and improving combustion performance.

4 Conclusion

In the present study, a detailed investigation is conducted on combustion regime diagrams, with a focus on the MILD combustion regime and its interaction with other regimes. Initially analyzed the border point of various combustion regime diagrams available in the literature. Based on the observation, the borderline between the MILD and no-combustion regimes results in the same magnitude of ignition delay time for a given fuel mixture. To further investigate a detailed analysis of a particular fuel under the influences of the various techniques available for stabilizing the flame in the MILD regime. Methane fuel is selected for the development of the combustion regime diagrams with the blending of hydrogen (50% volume) and influence by N_2, CO_2, H_2O, and EGR with the function of oxygen dilution and mixture temperature. A detailed analysis is conducted on the borderlines of the LL-MILD (interaction between no-combustion and MILD) and UL-MILD (interaction between the MILD and HiTAC). In addition to the criteria established in the literature for identifying the MILD combustion regime, an investigation is conducted by considered ignition delay time as a key parameter while emissions also keep into the account. An overlapped region is developed based on the LL-MILD and UL-MILD. The emissions of NO and CO are analyzed, and it is observed that lower NO and CO emissions are identified in the overlapped ignition delay times. In addition, O_2 influence on the various considered techniques for achieving the MILD combustion analyzed. The ranges of ignition delay times (overlapped region) are proposed for achieving the better combustion characteristics of MILD combustion. The proposed ranges of the ignition delay times are reported in Table 3.

Data availability statement

The raw data supporting the conclusions of this article will be made available by the authors, without undue reservation.

Author contributions

MS: Conceptualization, Data curation, Investigation, Software, Validation, Writing–original draft, Writing–review and editing. GS: Formal Analysis, Methodology, Writing–original draft, Writing–review and editing. VM: Resources, Software, Visualization, Writing–original draft, Writing–review and editing.

Funding

The author(s) declare that no financial support was received for the research, authorship, and/or publication of this article.

Acknowledgments

The authors would like to acknowledge the support from the Prime Minister Research Fellowship (PMRF) and the Indian Institute of Technology Kharagpur.

Conflict of interest

The authors declare that the research was conducted in the absence of any commercial or financial relationships that could be construed as a potential conflict of interest.

The author(s) declared that they were an editorial board member of Frontiers, at the time of submission. This had no impact on the peer review process and the final decision.

Generative AI statement

The author(s) declare that no Generative AI was used in the creation of this manuscript.

Publisher's note

References

Arghode, V. K., and Gupta, A. K. (2011). Development of high intensity CDC combustor for gas turbine engines. *Appl. Energy* 88, 963–973. doi:10.1016/j.apenergy.2010.07.038

Ariemma, G. B., Sorrentino, G., Sabia, P., Ragucci, R., and de Joannon, M. (2023). MILD combustion of methanol, ethanol and 1-butanol binary blends with ammonia. *Proc. Combust. Inst.* 39, 4509–4517. doi:10.1016/j.proci.2022.08.032

Bechtel, J. H. (1979). Temperature measurements of the hydroxyl radical and molecular nitrogen in premixed, laminar flames by laser techniques. *Appl. Opt.* 18 (13), 2100. doi:10.1364/AO.18.002100

Bechtel, J. H., Blint, R. J., Dasch, C. J., and Weinberger, D. A. (1981). Atmospheric pressure premixed hydrocarbon-air flames: theory and experiment. *Combust. Flame* 42, 197–213. doi:10.1016/0010-2180(81)90158-9

Cavaliere, A., and De Joannon, M. (2004). Mild combustion. *Prog. Energy Combust. Sci.* 30, 329–366. doi:10.1016/j.pecs.2004.02.003

Cavigiolo, A., Galbiati, M. A., Effuggi, A., Gelosa, D., and Rota, R. (2003). Mild combustion in a laboratory-scale apparatus. *Combust. Sci. Technol.* 175 (8), 1347–1367. doi:10.1080/00102200302356

Christo, F. C., and Dally, B. B. (2005). Modeling turbulent reacting jets issuing into a hot and diluted coflow. *Combust. Flame* 142, 117–129. doi:10.1016/j.combustflame.2005.03.002

Dally, B. B., Karpetis, A. N., and Barlow, R. S. (2002). Structure of turbulent non-premixed jet flames in a diluted hot coflow. *Proc. Combust. Inst.* 29 (1), 1147–1154. doi:10.1016/S1540-7489(02)80145-6

Darbyshire, O. R., and Swaminathan, N. (2012). A presumed joint pdf model for turbulent combustion with varying equivalence ratio. *Combust. Sci. Technol.* 184, 2036–2067. doi:10.1080/00102202.2012.696566

de Joannon, M., Sorrentino, G., and Cavaliere, A. (2012). MILD combustion in diffusion-controlled regimes of Hot Diluted Fuel. *Combust. Flame* 159, 1832–1839. doi:10.1016/j.combustflame.2012.01.013

Ebrahimi Fordoei, E., and Mazaheri, K. (2021). Effects of preheating temperature and dilution level of oxidizer, fuel composition and strain rate on NO emission characteristics in the syngas moderate or intense low oxygen dilution (MILD) combustion. *Fuel* 285, 119118. doi:10.1016/j.fuel.2020.119118

Galletti, C., Parente, A., and Tognotti, L. (2017). Numerical and experimental investigation of a mild combustion burner. *Combust. Flame* 151, 649–664. doi:10.1016/j.combustflame.2007.07.016

Garnayak, S., Elbaz, A. M., Kuti, O., Dash, S. K., Roberts, W. L., and Reddy, V. M. (2022). Auto-ignition and numerical analysis on high-pressure combustion of premixed methane-air mixtures in highly preheated and diluted environment. *Combust. Sci. Technol.* 194, 3132–3154. doi:10.1080/00102202.2021.1909579

Garnayak, S., Sharma, D., Dash, S. K., and Reddy, V. M. (2023). Numerical and chemical kinetic analyses on the formation of CO and CO2 for C1-C4 hydrocarbon alkanes in a hot Co-flow under MILD combustion. *Energy Fuels* 37, 2275–2293. doi:10.1021/acs.energyfuels.2c02700

Giuntini, L., Frascino, L., Ariemma, G. B., Galletti, C., Sorrentino, G., and Ragucci, R. (2023). Performance assessment of modeling approaches for moderate or intense low-oxygen dilution combustion in a scale-bridging burner. *Energy Fuels* 37, 9500–9513. doi:10.1021/acs.energyfuels.3c00597

Iavarone, S., and Parente, A. (2020). NO x formation in MILD combustion: potential and limitations of existing approaches in CFD. *Front. Mech. Eng.* 6, 13. doi:10.3389/fmech.2020.00013

Katsuki, M., and Hasegawa, T. (1998). The science and technology of combustion in highly preheated air. *Symp. Combust.* 27, 3135–3146. doi:10.1016/S0082-0784(98)80176-8

Kim, N., Kim, Y., Jaafar, M. N. M., Rahim, M. R., and Said, M. (2021). Effects of hydrogen addition on structure and NO formation of highly CO-Rich syngas counterflow nonpremixed flames under MILD combustion regime. *Int. J. Hydrogen Energy* 46, 10518–10534. doi:10.1016/j.ijhydene.2020.12.120

Kumar, S., Paul, P. J., and Mukunda, H. S. (2002). Studies on a new high-intensity low-emission burner. *Proc. Combust. Inst.* 29, 1131–1137. doi:10.1016/S1540-7489(02)80143-2

Mahendra Reddy, V., Sawant, D., Trivedi, D., and Kumar, S. (2013). Studies on a liquid fuel based two stage flameless combustor. *Proc. Combust. Inst.* 34, 3319–3326. doi:10.1016/j.proci.2012.06.028

Mardani, A., and Fazlollahi Ghomshi, A. (2016). Numerical study of oxy-fuel MILD (moderate or intense low-oxygen dilution combustion) combustion for CH4-H2 fuel. *Energy* 99, 136–151. doi:10.1016/j.energy.2016.01.016

Mardani, A., and Karimi Motaalegh Mahalegi, H. (2019). Hydrogen enrichment of methane and syngas for MILD combustion. *Int. J. Hydrogen Energy* 44, 9423–9437. doi:10.1016/j.ijhydene.2019.02.072

Mardani, A., and Tabejamaat, S. (2012). NOx formation in H2-CH4 blended flame under MILD conditions. *Combust. Sci. Technol.* 184 (7-8), 995–1010. doi:10.1080/00102202.2012.663991

Mardani, A., Tabejamaat, S., and Hassanpour, S. (2013). Numerical study of CO and CO2 formation in CH4/H2 blended flame under MILD condition. *Combust. Flame* 160, 1636–1649. doi:10.1016/j.combustflame.2013.04.003

Rao, A. G., and Levy, Y. (2010). "A new combustion methodology for low emission gas turbine engines," in 8th HiTACG Conference, January, 2010.

Reddy, V. M., Katoch, A., Roberts, W. L., and Kumar, S. (2015). Experimental and numerical analysis for high intensity swirl based ultra-low emission flameless combustor operating with liquid fuels. *Proc. Combust. Inst.* 35, 3581–3589. doi:10.1016/j.proci.2014.05.070

Sabia, P., de Joannon, M., Picarelli, A., and Ragucci, R. (2013). Methane auto-ignition delay times and oxidation regimes in MILD combustion at atmospheric pressure. *Combust. Flame* 160, 47–55. doi:10.1016/j.combustflame.2012.09.015

Sabia, P., de Joannon, M., Sorrentino, G., Giudicianni, P., and Ragucci, R. (2015). Effects of mixture composition, dilution level and pressure on auto-ignition delay times of propane mixtures. *Chem. Eng. J.* 277, 324–333. doi:10.1016/j.cej.2015.04.143

Sabia, P., Lubrano Lavadera, M., Sorrentino, G., Giudicianni, P., Ragucci, R., and de Joannon, M. (2016). H2O and CO2 dilution in MILD combustion of simple hydrocarbons. *Turbul. Combust.* 96, 433–448. doi:10.1007/s10494-015-9667-4

Sabia, P., Manna, M. V., Ariemma, G. B., Sorrentino, G., Ragucci, R., and de Joannon, M. (2023). Novel insights into mild combustion processes through analyses of hysteresis behavior. *Proc. Combust. Inst.* 39, 4501–4507. doi:10.1016/j.proci.2022.08.011

Sabia, P., Sorrentino, G., Ariemma, G. B., Manna, M. V., Ragucci, R., and de Joannon, M. (2021). MILD combustion and biofuels: a minireview. *Energy Fuels* 35, 19901–19919. doi:10.1021/acs.energyfuels.1c02973

Sharma, S., Pingulkar, H., Chowdhury, A., and Kumar, S. (2018). A new emission reduction approach in MILD combustion through asymmetric fuel injection. *Combust. Flame* 193, 61–75. doi:10.1016/j.combustflame.2018.03.008

Sorrentino, G., Göktolga, U., de Joannon, M., Van Oijen, J., Cavaliere, A., and De Goey, P. (2017). An experimental and numerical study of MILD combustion in a Cyclonic burner. *Energy Procedia* 120, 649–656. doi:10.1016/j.egypro.2017.07.173

Sorrentino, G., Sabia, P., Ariemma, G. B., Ragucci, R., and de Joannon, M. (2021). Reactive structures of ammonia MILD combustion in diffusion ignition processes. *Front. Energy Res.* 9. doi:10.3389/fenrg.2021.649141

Sorrentino, G., Sabia, P., de Joannon, M., Cavaliere, A., and Ragucci, R. (2016). The effect of diluent on the sustainability of MILD combustion in a cyclonic burner. *Turbul. Combust.* 96, 449–468. doi:10.1007/s10494-015-9668-3

Sorrentino, G., Sabia, P., de Joannon, M., Ragucci, R., Cavaliere, A., Göktolga, U., et al. (2015). Development of a novel cyclonic flow combustion chamber for achieving MILD/flameless combustion. *Phys. Procedia* 66, 141–144. doi:10.1016/j.egypro.2015.02.079

Srinivasarao, M., Jun, D., Jik, B., and Reddy, V. M. (2023). International Journal of Hydrogen Energy Numerical analysis of the enrichment of CH 4/H 2 in ammonia combustion in a hot co-flow environment. *Int. J. Hydrogen Energy*. doi:10.1016/j.ijhydene.2023.11.160

Srinivasarao, M., Lee, B. J., and Reddy, V. M. (2024). Modified reacting solver: a simplified approach for capturing the molecular and flow diffusivities for the nonpremixed MILD flames. *ACS Omega* 9, 15804–15817. doi:10.1021/acsomega.3c07212

Srinivasarao, M., and Reddy, V. M. (2024). Effect of thermodiffusion on non premixed flame in MILD regime using a modified reacting solver. *Solver* 74, 173–180. doi:10.14429/dsj.74.19627

Stephenson, D. A. (1979). Non-intrusive profiles of atmospheric premixed hydrocarbon-air flames. *Symp. (Int.) Combust.* 17 (1), 993–999. doi:10.1016/S0082-0784(79)80096-X

Tu, Y., Xu, S., Xu, M., Liu, H., and Yang, W. (2020). Numerical study of methane combustion under moderate or intense low-oxygen dilution regime at elevated pressure conditions up to 8 atm. *Energy* 197, 117158.

Wünning, J. A., and Wünning, J. G. (1997). Flameless oxidation to reduce thermal no-formation. *Prog. Energy Combust. Sci.* 23, 81–94. doi:10.1016/s0360-1285(97)00006-3

Yang, J., Zou, C., Li, W., Lin, Q., Lu, L., and Xia, W. (2022). Experimental and numerical study on the ignition delay times of dimethyl ether/propane mixtures in O2/CO2 atmospheres. *Fuel* 316, 123301. doi:10.1016/j.fuel.2022.123301